

# A Straightforward Strategy toward Large BN-Embedded $\pi$ -Systems: Synthesis, Structure, and Optoelectronic Properties of Extended BN Heterosuperbenzenes

Xiao-Ye Wang,<sup>†</sup> Fang-Dong Zhuang,<sup>†</sup> Rui-Bo Wang,<sup>†</sup> Xin-Chang Wang,<sup>‡</sup> Xiao-Yu Cao,<sup>\*,‡</sup> Jie-Yu Wang,<sup>\*,†</sup> and Jian Pei<sup>\*,†</sup>

<sup>†</sup>Beijing National Laboratory for Molecular Sciences, Key Laboratory of Bioorganic Chemistry and Molecular Engineering of Ministry of Education, College of Chemistry and Molecular Engineering, Peking University, Beijing 100871, China

<sup>‡</sup>College of Chemistry and Chemical Engineering, Xiamen University, Xiamen 361005, China

## Supporting Information

**ABSTRACT:** A straightforward strategy has been used to construct large BN-embedded  $\pi$ -systems simply from azaacenes. BN heterosuperbenzene derivatives, the largest BN heteroaromatics to date, have been synthesized in three steps. The molecules exhibit curved  $\pi$ -surfaces, showing two different conformations which are self-organized into a sandwich structure and further packed into a  $\pi$ -stacking column. The assembled microribbons exhibit good charge transport properties and photoconductivity, representing an important step toward the optoelectronic applications of BN-embedded aromatics.

Graphene is a two-dimensional (2D) honeycomb structure of carbon atoms. The zero-bandgap nature of graphene greatly hinders its application to electronic nanodevices as a semiconductor, thus triggering considerable efforts toward bandgap opening and engineering.<sup>1</sup> One of the promising approaches is chemical doping of graphene with heteroatoms.<sup>2</sup> Very recently, BN-doped graphene has emerged as a new type of single-layer 2D heterostructure with interesting electronic applications.<sup>3</sup> Many unusual physical properties were also revealed by theoretical studies.<sup>4</sup> However, only one type of BN-doped graphene with separate graphene and hexagonal boron nitride (h-BN) domains (Figure 1a) has been obtained. Another important doping type with controlled positions of individual BN units dispersed in the graphene framework (Figure 1b), which may possess distinct electronic properties and facilitate the understanding of the fundamental structure–property relationship, has never been created. This situation is

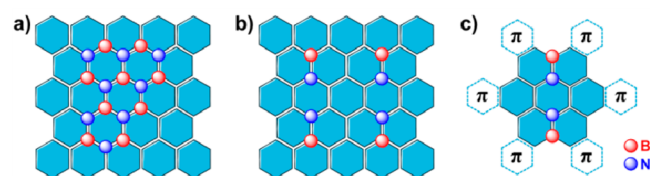


**Figure 1.** Schematic representations of substructures of BN-doped graphenes (a) with separate h-BN and graphene domains and (b) with individual BN units doped in the graphene framework. (c) The  $\pi$ -extended BN heterosuperbenzene synthesized in this work.

due to the theoretically predicted phase separation<sup>5</sup> of h-BN and graphene domains in the one-step chemical vapor deposition process and the limitation of the top-down etching technique in a two-step patterned regrowth procedure. In this context, the bottom-up organic synthesis provides new possibilities of obtaining such an unexplored heterostructure through synthesizing well-defined BN-doped graphene fragments as precursors for surface-assisted growth.<sup>6</sup>

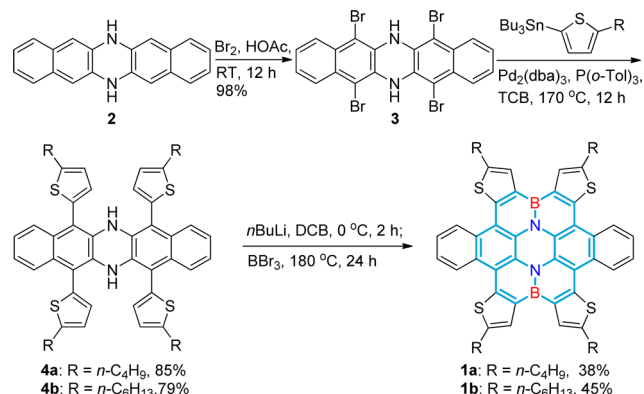
To this end, a simple and efficient synthetic approach to large BN heteroaromatics needs to be developed. Although significant progress has been made in azaborine chemistry,<sup>7,8</sup> the construction of polycyclic aromatics with BN inclusion, which was pioneered by Piers et al.,<sup>8c</sup> is still challenging and usually requires multiple steps or specific conditions.<sup>9</sup> Recently, Nakamura and co-workers developed a tandem electrophilic borylation method to efficiently synthesize BN-substituted polycyclic aromatics.<sup>9c</sup> However, an efficient approach to big 2D  $\pi$ -extended systems with more than one internalized BN unit is not well established, and the size achieved up to now is relatively small.<sup>9g</sup> Here, we use a straightforward strategy to construct large BN-embedded  $\pi$ -systems simply from azaacenes.  $\pi$ -Extended BN heterosuperbenzenes (Figure 1c) have been synthesized as a proof of concept. Considering the broad chemistry and diversity of azaacenes,<sup>10</sup> this strategy would be a general approach toward BN-doped graphene fragments and other large BN heteroarenes, which would also be interesting candidates for supramolecular chemistry and electronic devices,<sup>11</sup> providing new opportunities in the efforts to develop BN-containing  $\pi$ -conjugated materials.<sup>9</sup>

The synthetic route to **1a** and **1b** is illustrated in Scheme 1. 6,13-Dihydro-6,13-diazapentacene (**2**) was easily accessed from commercially available 2,3-dihydroxynaphthalene and 2,3-diaminonaphthalene.<sup>12</sup> Regioselective bromination of **2** with Br<sub>2</sub> gave compound **3** in nearly quantitative yield. A Stille coupling reaction between **3** and tributyl(5-alkylthiophen-2-yl)stannanes introduced four alkylthiophenes onto the azapentacene backbone, and an electrophilic borylation reaction<sup>9</sup> produced compounds **1a** and **1b** as yellow solids. This synthetic route is simple and straightforward, creating novel BN heterocoronene derivatives from azapentacene **2** in three steps.

Received: January 6, 2014

Published: March 2, 2014

## Scheme 1. Synthetic Route to 1a and 1b



Compounds **1a** and **1b** were characterized by <sup>1</sup>H, <sup>13</sup>C, and <sup>11</sup>B NMR, MALDI-TOF MS, and elemental analysis. Both compounds are stable to ambient conditions in solid state. Thermogravimetric analysis revealed decomposition temperatures (5% weight loss) of >450 °C. The photophysical and electrochemical properties of both compounds were also investigated (see Supporting Information). The absorption and emission features of **1a** and **1b** are identical in both solution and solid state. The obvious vibrational structure of **1b** indicates the rigidity of the skeleton. The optical bandgaps of **4b** and **1b**, estimated from the absorption onsets, were 2.70 and 2.59 eV, respectively. Compounds **4b** and **1b** showed quasi-reversible oxidative waves in cyclic voltammetry measurements. The HOMO energy levels were estimated to be -4.96 eV for **4b** and -5.07 eV for **1b**.

The molecular structure of **1b** was determined by single-crystal X-ray diffraction (XRD) (Figure 2). The BN bonds are around 1.46 Å, a typical bond length of the delocalized BN double bonds.<sup>13</sup> Owing to the steric hindrance among the peripheral rings, the aromatic core of **1b** is significantly distorted. Two different conformations were found in the same crystal, which is quite a rare phenomenon for polycyclic aromatics. The six peripheral rings adopt an up-down-down-up-down-down conformation (termed as saddle-shaped conformation A) and an up-down-up-down-up-down conformation (termed as alternately up-down conformation B). Conformers A and B coexist in a ratio of 2:1 in the crystal. In conformation A, as shown in Figure 2c, the azapentacene is bent to form an upward curvature, while in the perpendicular direction (along the B-N-N-B direction) an opposite curvature is formed. This negatively curved BN-embedded  $\pi$ -system<sup>14</sup> can be viewed as a good model to understand the curvature behavior in BN-doped carbon nanotubes and warped graphenes.<sup>15</sup> The single crystal shows a columnar stacking along the [011] direction (Figure S5). Interestingly, inside the column, conformer B is sandwiched between two conformers A (A1 and A2), which are symmetrical to each other, to form a basic packing unit. This A1-B-A2 sandwich structure is further packed into a  $\pi$ -stacking column. At the stacking interface of each unit, conformers A2 and A1 are closely stacked in a perpendicular manner due to the perfect match of the “double-concave” surfaces. In other words, each A1-B-A2 unit is stacked together with a rotation angle of about 90°. This self-organization process of the two conformers of one single compound is very interesting in supramolecular chemistry.

The effects of incorporating BN units into the  $\pi$ -conjugated backbone were studied by density functional theory (DFT) calculations (Figure 3). The geometries of both conformations A

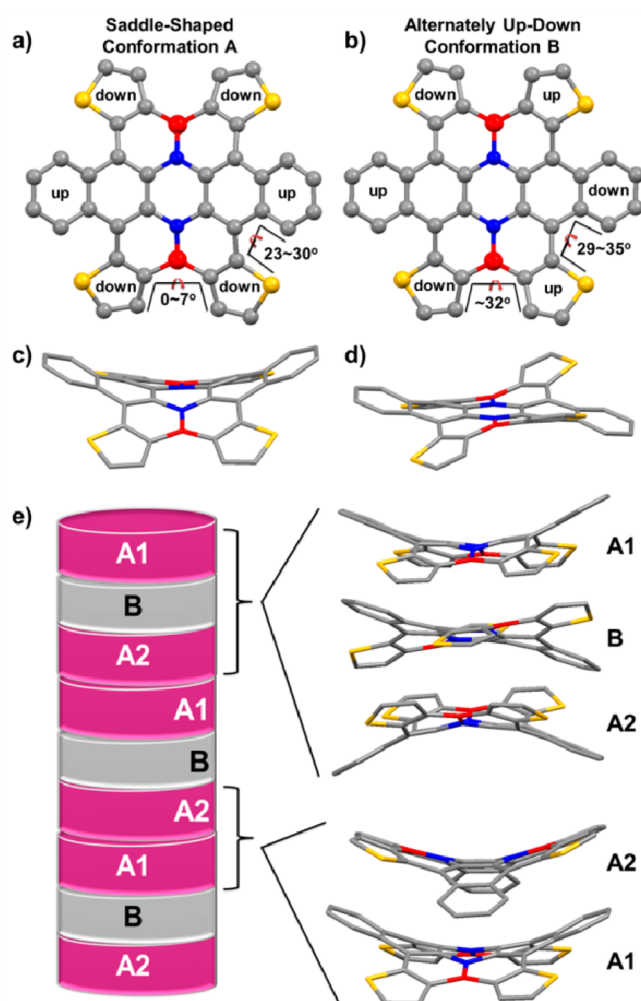


**Figure 2.** Single-crystal structure of **1b** with (a,b) top views and (c,d) side views of (a,c) the saddle-shaped conformation A and (b,d) the alternately up-down conformation B. (e) Graphic illustration of the columnar stacking structure with the dislocation information omitted. Hydrogen atoms and alkyl chains are omitted for clarity. Colors: gray, carbon; red, boron; blue, nitrogen; yellow, sulfur.

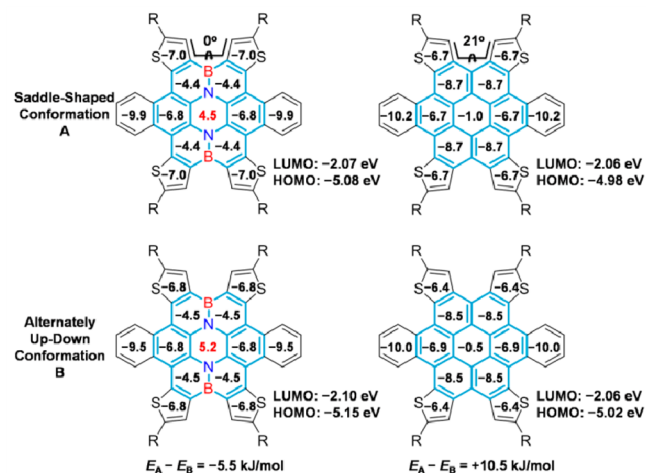


**Figure 3.** DFT-calculated results of the two conformers of both the BN-heterocoronene derivative and its carbon analogue. The energies were calculated at the B3LYP/6-311G(d,p) level. NICS(1) values were calculated at the GIAO-B3LYP/6-311+G(2,d,p) level.

and B of the BN heterocoronene derivative were optimized at the B3LYP/6-311G(d,p) level. The corresponding carbon-based dibenzotetrathienocoronene has not been reported, although a similar skeleton was developed by Nuckolls et al. recently with thiophene rings fused at the opposite position.<sup>16</sup> Therefore, for comparison, we just changed the BN units to CC units without altering their atomic coordinates, and then performed optimizations at the same level of theory. The incorporation of BN units changes the stable conformations (see Supporting Information) and electronic properties. For both conformers, the incorporation of BN units results in lowered HOMO levels by about 0.1 eV, while LUMO levels are almost unchanged. The lowered HOMO levels are beneficial to the air stability of these molecules as p-type semiconductors.<sup>17</sup> The enlarged bandgap demonstrates the efficacy of BN inclusion for bandgap opening of large  $\pi$ -systems. Nucleus-independent chemical shift (NICS) calculations<sup>18</sup> were performed to investigate the aromaticity of each ring. The central six-membered rings of the carbon analogue show very weak aromaticity, whereas the central  $N_2C_4$  six-membered rings of BN-heterocoronenes are antiaromatic, which may facilitate the doping process of large polycyclic aromatics.<sup>19</sup> These results indicate that the incorporation of BN units creates a new type of heteroarene with altered molecular geometries and electronic properties.

The strong aggregation tendency of compound **1b** in solution was evidenced by concentration-dependent <sup>1</sup>H NMR spectroscopy.<sup>20</sup> The signal of protons on the thiophene rings ( $H_a$ ) shifted upfield from 7.79 to 7.45 ppm as the concentration increased from 1 to 50 mM (Figure S6). Meanwhile, the signals of protons on the benzene rings ( $H_b$  and  $H_c$ ) also shifted upfield by about 0.50 and 0.37 ppm, respectively. Due to the strong intermolecular  $\pi$ - $\pi$  interactions, one-dimensional (1D) microribbons were obtained from a mixed solution of **1b** in  $CH_2Cl_2$ /EtOAc by slow evaporation, providing the possibility to evaluate the electrical properties of the new BN heterosuperbenzene derivative. Field-effect transistors (FETs) based on these microribbons were fabricated,<sup>21</sup> as illustrated in Figure 4a. A suspension of microribbons was spin-coated onto the CYTOP-modified  $SiO_2/Si$  substrates, and then the Au source and drain electrodes were evaporated with an organic ribbon mask.<sup>21a</sup> The scanning electron microscopy (SEM) image of the microribbon in the device configuration is shown in Figure 4b. To investigate the packing information inside the microribbons, transmission

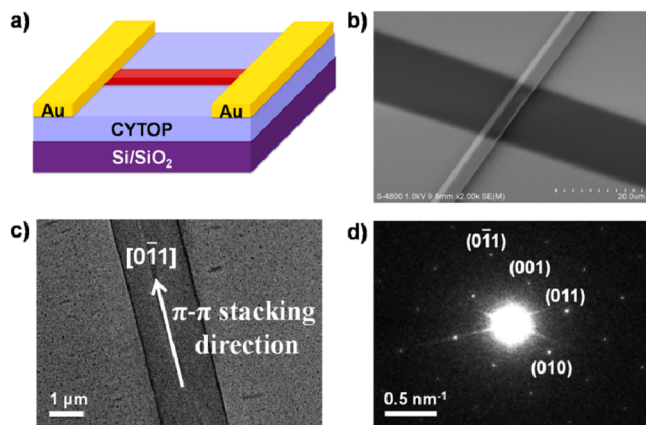


**Figure 4.** (a) Graphic illustration of the microribbon FET device of **1b**. (b) SEM image of the microribbon device. (c) TEM image of the microribbon and (d) its corresponding SAED pattern.

electron microscopy (TEM) and selected area electron diffraction (SAED) were performed (Figure 4c,d). The SAED pattern was indexed according to the single-crystal XRD data. The microribbons were grown along the  $[0\bar{1}1]$  direction, which is the columnar  $\pi$ - $\pi$  stacking direction. All devices exhibited p-channel characteristics, with the highest mobility of  $0.23 \text{ cm}^2 \text{ V}^{-1} \text{ s}^{-1}$ , a low threshold of  $-3 \text{ V}$ , and a current on/off ratio of  $>10^4$  (Figure 5). This performance is moderate but very impressive for

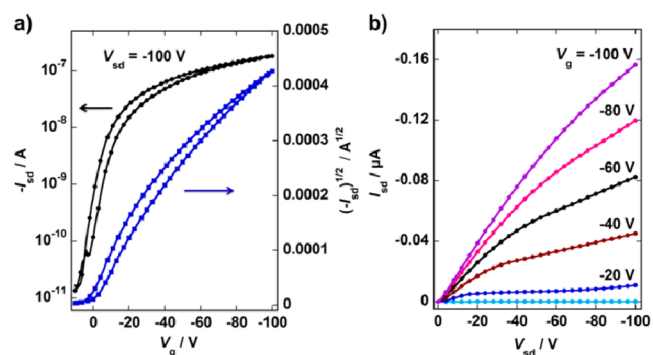


**Figure 5.** (a) Transfer and (b) output characteristics of the microribbon FET devices based on **1b**.

curved aromatics.<sup>22,23</sup> Further DFT investigations revealed that conformer B holds a higher reorganization energy of 368 meV, compared to conformer A (157 meV), which is detrimental to efficient charge transport. With crystal engineering strategies, such as eliminating conformers B in the crystal, the device performance may be further improved. The decent charge transport properties of these microribbons prompted us to investigate the photoresponsive electrical properties of BN heteroarenes. The conductivity was measured in the same device configuration in a two-wire resistor mode (see Supporting Information). Upon light irradiation, the current was enhanced significantly compared to the low conductivity under dark. These preliminary results demonstrate the great potential of BN heteroarenes for optoelectronic applications.<sup>24</sup>

In conclusion, a straightforward strategy has been used to construct BN heterosuperbenzene derivatives, the largest BN heteroaromatics reported to date. The incorporation of BN units has proven to be effective to modulate the electronic properties and molecular geometries of the  $\pi$ -conjugated backbone, creating a new type of heteroarenes. The unique crystal packing of the two different conformers of one single compound makes it an interesting example to investigate the molecular recognition and self-organization process in one-component system. Furthermore, the impressive FET performance among curved aromatics and the first demonstration of photoconductivity also represent an important step toward developing BN-containing  $\pi$ -conjugated materials. This general strategy to build large BN-embedded  $\pi$ -systems directly from azaacenes not only facilitates the synthesis of large BN heteroarenes with interesting properties for supramolecular chemistry and optoelectronic devices, but also opens up new possibilities to construct the unexplored type of BN-embedded graphene through a bottom-up synthetic approach.

## ■ ASSOCIATED CONTENT

### 📄 Supporting Information

Experimental details, synthesis, characterization, device fabrication and measurements, computational studies, and single-crystal



data (CIF). This material is available free of charge via the Internet at <http://pubs.acs.org>.

## AUTHOR INFORMATION

### Corresponding Authors

xcao@xmu.edu.cn

jiyuwang@pku.edu.cn

jianpei@pku.edu.cn

### Notes

The authors declare no competing financial interest.

## ACKNOWLEDGMENTS

This work was supported by the Major State Basic Research Development Program (No. 2013CB933501) from the Ministry of Science and Technology, and National Natural Science Foundation of China. The authors thank Dr. Hai Fu for help in single-crystal X-ray analysis.

## REFERENCES

- (1) (a) Geim, A. K.; Novoselov, K. S. *Nat. Mater.* **2007**, *6*, 183. (b) Novoselov, K. S.; Geim, A. K.; Morozov, S. V.; Jiang, D.; Zhang, Y.; Dubonos, S. V.; Grigorieva, I. V.; Firsov, A. A. *Science* **2004**, *306*, 666. (c) Jiao, L.; Zhang, L.; Wang, X.; Diankov, G.; Dai, H. *Nature* **2009**, *458*, 877. (d) Kosynkin, D. V.; Higginbotham, A. L.; Sinititskii, A.; Lomeda, J. R.; Dimiev, A.; Price, B. K.; Tour, J. M. *Nature* **2009**, *458*, 872.
- (2) (a) Wang, X.; Li, X.; Zhang, L.; Yoon, Y.; Weber, P. K.; Wang, H.; Guo, J.; Dai, H. *Science* **2009**, *324*, 768. (b) Tang, Y.-B.; Yin, L.-C.; Yang, Y.; Bo, X.-H.; Cao, Y.-L.; Wang, H.-E.; Zhang, W.-J.; Bello, I.; Lee, S.-T.; Cheng, H.-M.; Lee, C.-S. *ACS Nano* **2012**, *6*, 1970. (c) Liu, H.; Liu, Y.; Zhu, D. *J. Mater. Chem.* **2011**, *21*, 3335.
- (3) (a) Ci, L. J.; Song, L.; Jin, C.; Jariwala, D.; Wu, D.; Li, Y.; Srivastava, A.; Wang, Z. F.; Storr, K.; Balicas, L.; Liu, F.; Ajayan, P. M. *Nat. Mater.* **2010**, *9*, 430. (b) Levendoff, M. P.; Kim, C. J.; Brown, L.; Huang, P. Y.; Havener, R. W.; Muller, D. A.; Park, J. W. *Nature* **2012**, *488*, 627. (c) Liu, Z.; Ma, L.; Shi, G.; Zhou, W.; Gong, Y.; Lei, S.; Yang, X.; Zhang, J.; Yu, J.; Hackenberg, K. P.; Babakhani, A.; Idrobo, J.-C.; Vajtai, R.; Lou, J.; Ajayan, P. M. *Nat. Nanotechnol.* **2013**, *8*, 119.
- (4) (a) Ramasubramanian, A.; Naveh, D. *Phys. Rev. B* **2011**, *84*, 075405. (b) Jiang, J.-W.; Wang, J.-S.; Wang, B.-S. *Appl. Phys. Lett.* **2011**, *99*, 043109. (c) Zhao, R.; Wang, J.; Yang, M.; Liu, Z.; Liu, Z. *J. Phys. Chem. C* **2012**, *116*, 21098.
- (5) Zhu, J.; Bhandary, S.; Sanyal, B.; Ottosson, H. *J. Phys. Chem. C* **2011**, *115*, 10264.
- (6) (a) Wu, J.; Pisula, W.; Müllen, K. *Chem. Rev.* **2007**, *107*, 718. (b) Chen, L.; Hernandez, Y.; Feng, X.; Müllen, K. *Angew. Chem., Int. Ed.* **2012**, *51*, 7640. (c) Yan, X.; Li, B.; Li, L.-S. *Acc. Chem. Res.* **2013**, *46*, 2254. (d) Cai, J.; Ruffieux, P.; Jaafar, R.; Bieri, M.; Braun, T.; Blankenburg, S.; Muoth, M.; Seitsonen, A. P.; Saleh, M.; Feng, X.; Müllen, K.; Fasel, R. *Nature* **2010**, *466*, 470. (e) Qian, H.; Negri, F.; Wang, C.; Wang, Z. *J. Am. Chem. Soc.* **2008**, *130*, 17970.
- (7) For reviews, see: (a) Campbell, P. G.; Marwitz, A. J. V.; Liu, S.-Y. *Angew. Chem., Int. Ed.* **2012**, *51*, 6074. (b) Bosdet, M. J. D.; Piers, W. E. *Can. J. Chem.* **2009**, *87*, 8. (c) Liu, Z.; Marder, T. B. *Angew. Chem., Int. Ed.* **2008**, *47*, 242.
- (8) For representative examples, see: (a) Abbey, E. R.; Lamm, A. N.; Baggett, A. W.; Zakharov, L. N.; Liu, S.-Y. *J. Am. Chem. Soc.* **2013**, *135*, 12908. (b) Lu, J. S.; Ko, S. B.; Walters, N. R.; Kang, Y.; Sauriol, F.; Wang, S. *Angew. Chem., Int. Ed.* **2013**, *52*, 4544. (c) Jaska, C. A.; Emslie, D. J. H.; Bosdet, M. J. D.; Piers, W. E.; Sorensen, T. S.; Parvez, M. *J. Am. Chem. Soc.* **2006**, *128*, 10885. (d) Bosdet, M. J. D.; Piers, W. E.; Sorensen, T. S.; Parvez, M. *Angew. Chem., Int. Ed.* **2007**, *46*, 4940. (e) Ashe, A. J., III; Fang, X. *Org. Lett.* **2000**, *2*, 2089. (f) Taniguchi, T.; Yamaguchi, S. *Organometallics* **2010**, *29*, 5732.
- (9) For recent examples on BN-substituted  $\pi$ -conjugated materials, see: (a) Neue, B.; Aranedo, J. F.; Piers, W. E.; Parvez, M. *Angew. Chem., Int. Ed.* **2013**, *52*, 9966. (b) Lepeltier, M.; Lukoyanova, O.; Jacobson, A.; Jeeva, S.; Perepichka, D. F. *Chem. Commun.* **2010**, *46*, 7007.
- (c) Hatakeyama, T.; Hashimoto, S.; Seki, S.; Nakamura, M. *J. Am. Chem. Soc.* **2011**, *133*, 18614. (d) Hatakeyama, T.; Hashimoto, S.; Oba, T.; Nakamura, M. *J. Am. Chem. Soc.* **2012**, *134*, 19600. (e) Wang, X.-Y.; Lin, H.-R.; Lei, T.; Yang, D.-C.; Zhuang, F.-D.; Wang, J.-Y.; Yuan, S.-C.; Pei, J. *Angew. Chem., Int. Ed.* **2013**, *52*, 3117. (f) Wang, X.; Zhang, F.; Liu, J.; Tang, R.; Fu, Y.; Wu, D.; Xu, Q.; Zhuang, X.; He, G.; Feng, X. *Org. Lett.* **2013**, *15*, 5714. (g) Bosdet, M. J. D.; Piers, W. E.; Sorensen, T. S.; Parvez, M. *Can. J. Chem.* **2010**, *88*, 426.
- (10) For reviews, see: (a) Anthony, J. E. *Chem. Rev.* **2006**, *106*, 5028. (b) Miao, Q. *Synlett* **2012**, *23*, 326. (c) Bunz, U. H. F.; Engelhart, J. U.; Lindner, B. D.; Schaffroth, M. *Angew. Chem., Int. Ed.* **2013**, *52*, 3810.
- (11) (a) Zhang, W.; Jin, W.; Fukushima, T.; Saeki, A.; Seki, S.; Aida, T. *Science* **2011**, *334*, 340. (b) Kang, S. J.; Ahn, S.; Kim, J. B.; Schenck, C.; Hiszpanski, A. M.; Oh, S.; Schiros, T.; Loo, Y.-L.; Nuckolls, C. *J. Am. Chem. Soc.* **2013**, *135*, 2207. (c) Chen, L.; Mali, K. S.; Puniredd, S. R.; Baumgarten, M.; Parvez, K.; Pisula, W.; Feyter, S. D.; Müllen, K. *J. Am. Chem. Soc.* **2013**, *135*, 13531.
- (12) Miao, Q.; Nguyen, T.-Q.; Someya, T.; Blanchet, G. B.; Nuckolls, C. *J. Am. Chem. Soc.* **2003**, *125*, 10284.
- (13) Abbey, E. R.; Zakharov, L. N.; Liu, S.-Y. *J. Am. Chem. Soc.* **2008**, *130*, 7250.
- (14) For recent reports on all-carbon, negatively curved  $\pi$ -systems, see: (a) Kawasumi, K.; Zhang, Q.; Segawa, Y.; Scott, L. T.; Itami, K. *Nat. Chem.* **2013**, *5*, 739. (b) Feng, C.-N.; Kuo, M.-Y.; Wu, Y.-T. *Angew. Chem., Int. Ed.* **2013**, *52*, 7791. (c) Sakamoto, Y.; Suzuki, T. *J. Am. Chem. Soc.* **2013**, *135*, 14074. (d) Luo, J.; Xu, X.; Mao, R.; Miao, Q. *J. Am. Chem. Soc.* **2012**, *134*, 13796.
- (15) Kim, S. Y.; Park, J.; Choi, H. C.; Ahn, J. P.; Hou, J. Q.; Kang, H. S. *J. Am. Chem. Soc.* **2007**, *129*, 1705.
- (16) (a) Gorodetsky, A. A.; Chiu, C.-Y.; Schiros, T.; Palma, M.; Cox, M.; Jia, Z.; Sattler, W.; Kymissis, I.; Steigerwald, M.; Nuckolls, C. *Angew. Chem., Int. Ed.* **2010**, *49*, 7909. (b) Chiu, C.-Y.; Kim, B.; Gorodetsky, A. A.; Sattler, W.; Wei, S. J.; Sattler, A.; Steigerwald, M.; Nuckolls, C. *Chem. Sci.* **2011**, *2*, 1480. (c) Kang, S. J.; Kim, J. B.; Chiu, C.-Y.; Ahn, S.; Schiros, T.; Lee, S. S.; Yager, K. G.; Toney, M. F.; Loo, Y.-L.; Nuckolls, C. *Angew. Chem., Int. Ed.* **2012**, *51*, 8594.
- (17) Wang, C.; Dong, H.; Hu, W.; Liu, Y.; Zhu, D. *Chem. Rev.* **2012**, *112*, 2208.
- (18) Chen, Z.; Wannere, C. S.; Corminboeuf, C.; Puchta, R.; Schleyer, P. v. R. *Chem. Rev.* **2005**, *105*, 3842.
- (19) (a) Xiao, S.; Kang, S. J.; Zhong, Y.; Zhang, S.; Scott, A. M.; Moscatelli, A.; Turro, N. J.; Steigerwald, M. L.; Li, H.; Nuckolls, C. *Angew. Chem., Int. Ed.* **2013**, *52*, 4558. (b) Takase, M.; Narita, T.; Fujita, W.; Asano, M. S.; Nishinaga, T.; Bente, H.; Yoza, K.; Müllen, K. *J. Am. Chem. Soc.* **2013**, *135*, 8031.
- (20) Zou, L.; Wang, X.-Y.; Shi, K.; Wang, J.-Y.; Pei, J. *Org. Lett.* **2013**, *15*, 4378.
- (21) (a) Tang, Q.; Jiang, L.; Tong, Y.; Li, H.; Liu, Y.; Wang, Z.; Hu, W.; Liu, Y.; Zhu, D. *Adv. Mater.* **2008**, *20*, 2947. (b) Briseno, A. L.; Mannsfeld, S. C. B.; Jenekhe, S. A.; Bao, Z.; Xia, Y. *Mater. Today* **2008**, *11*, 38. (c) Jiang, W.; Zhou, Y.; Geng, H.; Jiang, S.; Yan, S.; Hu, W.; Wang, Z.; Shuai, Z.; Pei, J. *J. Am. Chem. Soc.* **2011**, *133*, 1.
- (22) The mobilities of reported curved aromatics are generally in the range of  $10^{-5}$ – $10^{-2}$   $\text{cm}^2 \text{V}^{-1} \text{s}^{-1}$ . See refs 14c,d and (a) Xiao, S.; Tang, J.; Beetz, T.; Guo, X.; Tremblay, N.; Siegrist, T.; Zhu, Y.; Steigerwald, M.; Nuckolls, C. *J. Am. Chem. Soc.* **2006**, *128*, 10700. (b) Xiao, S.; Ju, Kang, S.; Wu, Y.; Ahn, S.; Kim, J. B.; Loo, Y.-L.; Siegrist, T.; Steigerwald, M. L.; Li, H.; Nuckolls, C. *Chem. Sci.* **2013**, *4*, 2018.
- (23) A mobility of about  $1 \text{ cm}^2 \text{V}^{-1} \text{s}^{-1}$  was estimated on the basis of contorted hexabenzocoronenes in a monolayer transistor with extremely narrow channel lengths (2–6 nm) using carbon nanotube electrodes. See: Guo, X.; Myers, M.; Xiao, S.; Lefenfeld, M.; Steiner, R.; Tulevski, G. S.; Tang, J.; Baumert, J.; Leibfarth, F.; Yardley, J. T.; Steigerwald, M. L.; Kim, P.; Nuckolls, C. *Proc. Natl. Acad. Sci. U.S.A.* **2006**, *103*, 11452.
- (24) Dong, H.; Zhu, H.; Meng, Q.; Gong, X.; Hu, W. *Chem. Soc. Rev.* **2012**, *41*, 1754.